

Nonquasiparticle states in half-metallic ferromagnets

V. Yu. Irkhin¹, M. I. Katsnelson², and A. I. Lichtenstein³

¹Institute of Metal Physics, 620219, Ekaterinburg, Russia

²Department of Physics, Uppsala University, Box 530, SE-751 21 Uppsala, Sweden

³Institute of Theoretical Physics, University of Hamburg, Jungiusstrasse 9, 20355 Hamburg, Germany

Summary. Anomalous magnetic and electronic properties of the half-metallic ferromagnets (HMF) have been discussed. The general conception of the HMF electronic structure which take into account the most important correlation effects from electron-magnon interactions, in particular, the spin-polaron effects, is presented. Special attention is paid to the so called non-quasiparticle (NQP) or incoherent states which are present in the gap near the Fermi level and can give considerable contributions to thermodynamic and transport properties. Prospects of experimental observation of the NQP states in core-level spectroscopy is discussed. Special features of transport properties of the HMF which are connected with the absence of one-magnon spin-flip scattering processes are investigated. The temperature and magnetic field dependences of resistivity in various regimes are calculated. It is shown that the NQP states can give a dominate contribution to the temperature dependence of the impurity-induced resistivity and in the tunnel junction conductivity. First principle calculations of the NQP-states for the prototype half-metallic material NiMnSb within the local-density approximation plus dynamical mean field theory (LDA+DMFT) are presented.

1 Introduction

Half-metallic ferromagnets (HMF) [1, 2, 3] attract recently a great scientific and industrial attentions due to their importance for spin-dependent electronics or “spintronics” [4]. The HMF have metallic electronic structure for one spin projection (majority- or minority-spin states), but for the opposite spin direction the Fermi level lies in the energy gap [1]. Therefore the spin-up and spin-down contributions to electronic transport properties have different orders of magnitude, which can result in a huge magnetoresistance for heterostructures containing the HMF [2].

At the same time, the HMF are very interesting conceptually as a class of materials which may be suitable for investigation of the essentially many-body physics “beyond standard band theory”. In the most cases many-body effects lead only to renormalization of the quasiparticle parameters in the sense of Landau’s Fermi liquid theory, the electronic *liquid* being *qualitatively* similar to the electron *gas* (see, e.g., [5, 6]). On the other hand, due to specific

band structure of the HMF, an important role belongs here to incoherent (nonquasiparticle, NQP) states which occur near the Fermi level because of correlation effects [2]. The appearance of NQP states in the energy gap near the Fermi level is one of the most interesting correlation effects typical for the HMF. The origin of these states is connected with “spin-polaron” processes: the spin-down low-energy electron excitations, which are forbidden for the HMF in standard one-particle scheme, turn out to be possible as superpositions of spin-up electron excitations and virtual magnons. The density of these nonquasiparticle states vanishes at the Fermi level, but increases drastically at the energy scale of the order of a characteristic magnon frequency $\bar{\omega}$. The NQP states were first considered theoretically by Edwards and Hertz [7] in the framework of a broad-band Hubbard model for itinerant electron ferromagnets. Later it was demonstrated [8] that for a *narrow-band* (infinite- U) Hubbard model the *whole* spectral weight for one spin projection belongs to the NQP states which is of crucial importance for the problem of stability of Nagaoka’s ferromagnetism [9] and for adequate description of corresponding excitation spectrum. The NQP states in the $s-d$ exchange model of magnetic semiconductors have been considered in Ref. [10]. It was shown that depending on the sign of the $s-d$ exchange integral, the NQP states can form either only below the Fermi energy E_F or only above it. Later it was realized that the HMF are natural substances for theoretical and experimental investigating of the NQP effects [11]. A variety of these effects in the electronic and magnetic properties has been considered (for review of the earlier works see Ref. [2]) and some recent developments will be discussed in the present paper. As an example of highly unusual properties of the NQP states, we note that they can contribute to the T -linear term in the electron heat capacity [11, 12], despite their density at E_F vanishes at temperature $T = 0$. Existence of the NQP states at the HMF surface has been predicted in Ref. [13] and may be important for their detection by surface-sensitive methods such as the ARPES [14] or by spin-polarized scanning tunneling microscopy [15]. Recently the density of NQP states has been calculated from first principles for a prototype HMF, NiMnSb [16]. Some effects of the NQP states on physical properties of the HMF will be considered below. Because of the volume restrictions we will concentrate on several examples skipping the temperature dependence of nuclear magnetic relaxation rate [17] and many others.

2 Origin of nonquasiparticle states and electron spin polarization in the gap

From theoretical point of view, the HMF are characterized by the absence of magnons decay into the Stoner excitations (pairs electron-hole with the opposite spins). Therefore spin waves are well defined in the whole Brillouin zone, similar to the Heisenberg ferromagnets and degenerate ferromagnetic semiconductors. Thus, unlike for the usual itinerant ferromagnets, effects of

electron-magnon interactions (so-called spin-polaron effects) are not masked by the Stoner excitations in the HMF and may be studied in a “pure” form. As we will see below, the electron-magnon scattering results in the occurrence of NQP states.

We start our consideration of the interaction of charge carriers with local moments in the standard s - d exchange model [18]. The s - d exchange Hamiltonian reads

$$\mathcal{H} = \sum_{\mathbf{k}\sigma} t_{\mathbf{k}} c_{\mathbf{k}\sigma}^\dagger c_{\mathbf{k}\sigma} - \sum_{\mathbf{q}\mathbf{k}} I_{\mathbf{k},\mathbf{k}+\mathbf{q}} \sum_{\alpha\beta} \mathbf{S}_{\mathbf{q}} c_{\mathbf{k}\alpha}^\dagger \boldsymbol{\sigma}_{\alpha\beta} c_{\mathbf{k}-\mathbf{q}\beta} - \sum_{\mathbf{q}} J_{\mathbf{q}} \mathbf{S}_{\mathbf{q}} \mathbf{S}_{-\mathbf{q}} \quad (1)$$

where $c_{\mathbf{k}\sigma}^\dagger$, $c_{\mathbf{k}\sigma}$ and $\mathbf{S}_{\mathbf{q}}$ are operators for conduction electrons and localized spins in the quasimomentum representation, the electron spectrum $t_{\mathbf{k}}$ is referred to the Fermi level E_F , $I_{\mathbf{k},\mathbf{k}+\mathbf{q}}$ is the s - d exchange parameter, $\boldsymbol{\sigma}$ are the Pauli matrices. We include in the Hamiltonian explicitly the “direct” d - d exchange interaction (last term in Eq.(1)) to construct perturbation theory in a convenient form. In real materials, this interaction may have a superexchange nature or result from the indirect exchange via conduction electrons (in the HMF situation, this is not reduced to the RKKY interaction). In the latter case, the d - d exchange interaction comes from the same s - d interaction and cannot be considered as an independent parameter. However, as demonstrated by direct calculations (see e.g. Refs.[10, 19]), the corresponding terms with magnon frequencies occur in higher order of the I perturbations, for the case where the bare d - d exchange interaction is absent.

The s - d exchange model does not describe properly the electronic structure for such HMF as the Heusler alloys or CrO_2 , where there is no domination of the sp -electrons in electronic transport, and a separation of electrons into a localized d -like and a delocalized s -like group is questionable. In such a case, the Hubbard model which describes the Coulomb correlations in a d -band is more appropriate. However, qualitative effects of electron-magnon interaction do not depend on the microscopic model. The calculations of the electron and magnon Green’s functions in the non-degenerate Hubbard model were performed in Refs. [7, 11] and gave practically the same result as the s - d exchange model with simple replacement of I by the Hubbard parameter U .

As demonstrated by analysis of the electron-spin coupling, the NQP picture turns out to be different for two possible signs of the $s - d$ exchange parameter I . For $I < 0$ case, the spin-up NQP states appears below the Fermi level as an isolated region in the energy diagram (Fig. 1). The occupied states with the total spin $S - 1$ are a superposition of the states $|S\rangle|\downarrow\rangle$ and $|S - 1\rangle|\uparrow\rangle$. The entanglement of the states of electron and spin subsystems which is necessary to form the NQP states is a purely quantum effect formally disappearing at $S \rightarrow \infty$. For qualitative understanding why the NQP states are formed only below the E_F in this case, we consider a limit $I \rightarrow -\infty$. Then the charge carrier is really a many-body state of the

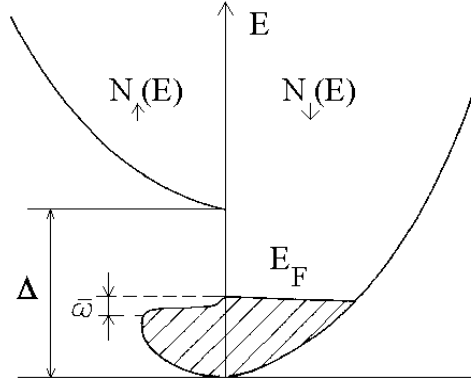


Fig. 1. Density of states in a half-metallic ferromagnet with $I < 0$ (schematically). Non-quasiparticle states with $\sigma = \uparrow$ occur below the Fermi level.

occupied site with total spin $S - 1/2$, which propagates in the ferromagnetic medium with spin S at any other site. The fractions of the states $|S\rangle|\downarrow\rangle$ and $|S - 1\rangle|\uparrow\rangle$ in the charge mobile carrier state are $1/(2S + 1)$ and $2S/(2S + 1)$, respectively, so that the first number is just a spectral weight of *occupied* spin-up electron NQP states. At the same time, the density of *empty* states is measured by the number of electrons with a given spin projection which can be added to the system. It is obvious that one cannot put any spin-up electrons in the spin-up site with $I = -\infty$. Therefore the density of NQP states should vanish above the E_F .

On the contrary, for the $I > 0$ case, the spin-down NQP scattering states form a “tail” of the upper spin-down band, which starts from the E_F (Fig. 2) since the Pauli principle prevents electron scattering into occupied states. A similar analysis of the limit $I \rightarrow +\infty$ helps to understand the situation qualitatively.

It is worthwhile to note that in the most known HMF energy gap exists for minority-spin states [2] which is similar to the case $I > 0$, therefore the NQP states should arise *above* the Fermi energy. For exceptional cases with the *majority*-spin gap such as a double perovskite $\text{Sr}_2\text{FeMoO}_6$ [20] one should expect the NQP states *below* the Fermi energy. This would be very interesting since in the latter case the NQP states can be probed by spin-polarized photoemission which is technically much simpler than spin-polarized BIS spectra [21] needed to probe the empty NQP states.

Let us consider now the density of states (DOS) scheme for the HMF within the $s - d$ exchange model more quantitatively [2, 10]. Neglecting the \mathbf{k} -dependence of $s - d$ exchange interaction, the electron Green’s function has the following form

$$G_{\mathbf{k}}^{\sigma}(E) = [E - t_{\mathbf{k}\sigma} - \Sigma_{\mathbf{k}\sigma}(E)]^{-1} \quad (2)$$

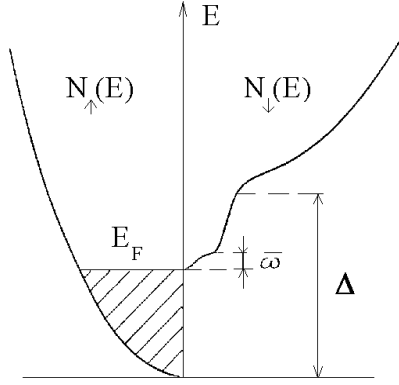


Fig. 2. Density of states in a half-metallic ferromagnet with $I > 0$ (schematically). Non-quasiparticle states with $\sigma = \downarrow$ occur above the Fermi level.

where $t_{\mathbf{k}\sigma} = t_{\mathbf{k}} - \sigma I \langle S^z \rangle$ is the mean-field electron spectrum and $\Sigma_{\mathbf{k}\sigma}(E)$ is the self-energy which describe the electron-magnon interactions. Within the second order approximation in I one has $\Sigma_{\mathbf{k}\sigma}(E) = 2I^2 S Q_{\mathbf{k}}^{\sigma}(E)$ with

$$Q_{\mathbf{k}}^{\uparrow}(E) = \sum_{\mathbf{q}} \frac{N_{\mathbf{q}} + n_{\mathbf{k}+\mathbf{q}}^{\downarrow}}{E - t_{\mathbf{k}+\mathbf{q}\downarrow} + \omega_{\mathbf{q}}}, \quad Q_{\mathbf{k}}^{\downarrow}(E) = \sum_{\mathbf{q}} \frac{1 + N_{\mathbf{q}} - n_{\mathbf{k}-\mathbf{q}}^{\uparrow}}{E - t_{\mathbf{k}-\mathbf{q}\uparrow} - \omega_{\mathbf{q}}} \quad (3)$$

Below we will present more accurate results for the Green's functions (see Eq.(29)) but here the lowest-order perturbation expression (3) will be sufficient.

Using an expansion of the Dyson equation (2) we obtain a simple expression for the electron DOS ($-\frac{1}{\pi} \text{Im} \sum_{\mathbf{k}} G_{\mathbf{k}\sigma}(E)$)

$$N_{\sigma}(E) = \sum_{\mathbf{k}} \delta(E - t_{\mathbf{k}\sigma}) - \sum_{\mathbf{k}} \delta'(E - t_{\mathbf{k}\sigma}) \text{Re} \Sigma_{\mathbf{k}\sigma}(E) - \frac{1}{\pi} \sum_{\mathbf{k}} \frac{\text{Im} \Sigma_{\mathbf{k}\sigma}(E)}{(E - t_{\mathbf{k}\sigma})^2} \quad (4)$$

The second term in the right-hand side of Eq. (4) describes the renormalization of quasiparticle energies. The third term, which arises from the branch cut of the self-energy $\Sigma_{\mathbf{k}\sigma}(E)$, describes the incoherent (nonquasiparticle) contribution owing to scattering by magnons. One can see that the NQP does not vanish in the energy region, corresponding to the “alien” spin subband with the opposite projection $-\sigma$. Substituting Eq.(3) into Eq.(4) and neglecting the quasiparticle shift we obtain for the case of HMF with $I > 0$

$$N_{\uparrow}(E) = \sum_{\mathbf{k}\mathbf{q}} \left[1 - \frac{2I^2 S N_{\mathbf{q}}}{(t_{\mathbf{k}+\mathbf{q}\downarrow} - t_{\mathbf{k}\uparrow})^2} \right] \delta(E - t_{\mathbf{k}\uparrow})$$

$$N_{\downarrow}(E) = 2I^2 S \sum_{\mathbf{k}\mathbf{q}} \frac{1 + N_{\mathbf{q}} - n_{\mathbf{k}\uparrow}}{(t_{\mathbf{k}+\mathbf{q}\downarrow} - t_{\mathbf{k}\uparrow} - \omega_{\mathbf{q}})^2} \delta(E - t_{\mathbf{k}\uparrow} - \omega_{\mathbf{q}}) \quad (5)$$

The DOS for case of the empty conduction band is shown in Fig.3. The $T^{3/2}$ -dependence of the magnon contribution to the residue of the Green's function (2), which follows from (3), i.e. of the effective electron mass in the lower spin subband, and an increase with temperature of the incoherent tail from the upper spin subband result in a strong temperature dependence of partial densities of states $N_\sigma(E)$, the corrections being of opposite sign.

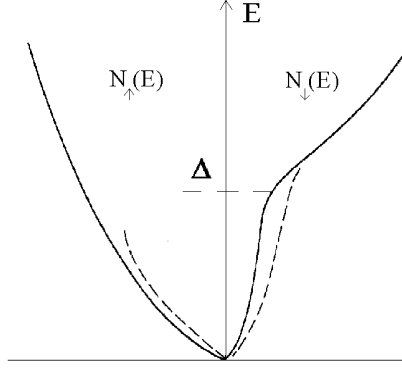


Fig. 3. Density of states in the s-d model in the case of empty conduction band ($I > 0$). At $T = 0$ (solid line) the spin-polaron tail of spin-down states reaches the band bottom. The dashed line corresponds to finite temperatures.

The behaviour of $N(E)$ near the Fermi level in the HMF (or degenerate ferromagnetic semiconductor) turns out to be also non-trivial (Figs. 2,3). If we neglect magnon frequencies in the denominators of Eq.(5), the partial density of incoherent states should occur as a jump above or below the Fermi energy E_F for the case of $I > 0$ and $I < 0$ respectively owing to the Fermi distribution functions. An account of finite magnon frequencies $\omega_{\mathbf{q}} = Dq^2$ (D is the spin stiffness constant) leads to the smearing of these singularities on the energy interval $\bar{\omega} \ll E_F$, with the $N(E_F)$ being equal to zero. For $|E - E_F| \ll \bar{\omega}$ we obtain

$$\frac{N_{-\alpha}(E)}{N_{\alpha}(E)} = \frac{1}{2S} \left| \frac{E - E_F}{\bar{\omega}} \right|^{3/2} \theta(\alpha(E - E_F)), \quad (6)$$

where $\alpha = \text{sign}(I) = \pm 1$ is the spin projections \uparrow, \downarrow of corresponding NQP-states. With increasing $|E - E_F|$, $N_{-\alpha}/N_{\alpha}$ tends to a constant value which is of order of I^2 within the perturbation theory. In the strong coupling limit where $|I| \rightarrow \infty$ we have for the $|E - E_F| \gg \bar{\omega}$

$$\frac{N_{-\alpha}(E)}{N_{\alpha}(E)} = \frac{1}{2S} \theta(\alpha(E - E_F)) \quad (7)$$

In a simple s - d model case, qualitative considerations [24], as well the Green's functions calculations [10, 25], gives a spin polarization of conduction electrons in the spin-wave region proportional to magnetization:

$$P \equiv \frac{N_{\uparrow} - N_{\downarrow}}{N_{\uparrow} + N_{\downarrow}} = 2P_0 \langle S^z \rangle \quad (8)$$

A weak ground-state depolarization $1 - P_0$ occurs in the case of $I > 0$. The behavior $P(T) \simeq \langle S^z \rangle$ is qualitatively confirmed by experimental data on field emission for ferromagnetic semiconductors [22] and transport properties for the half-metallic Heusler alloys [23]. Note, that the Eq. 8 is valid for a hole spin-wave region only for the narrow-band case (large I), whereas for the case of a small I it described spin-polarization only for very low temperatures.

An attempt to generalize the result (8) to the HMF case have been made on the basis of qualitative arguments for the atomic limit [26]. We will demonstrate that the situation for the HMF is more complicated. Let us focus on the magnon contribution to the DOS (5) and calculate a following function:

$$\Phi = \sum_{\mathbf{k}\mathbf{q}} \frac{2I^2 S N_{\mathbf{q}}}{(t_{\mathbf{k}+\mathbf{q}\downarrow} - t_{\mathbf{k}\uparrow} - \omega_{\mathbf{q}})^2} \delta(E_F - t_{\mathbf{k}\uparrow}) \quad (9)$$

Using the parabolic electron spectrum $t_{\mathbf{k}\uparrow} = k^2/2m$ and averaging over angles of the vector \mathbf{k} , we obtain

$$\Phi = \frac{2I^2 S m^2}{k_F^2} \rho \sum_{\mathbf{q}} \frac{N_{\mathbf{q}}}{(q^*)^2 - q^2}, \quad (10)$$

where $\rho = N_{\uparrow}(E_F, T = 0)$. We have used the condition $q \ll k_F$, $q^* = m\Delta/k_F = \Delta/v_F$, where $\Delta = 2|I|S$ is the spin splitting. Corresponding crossover energy scale is equal to $T^* = D(q^*)^2 \sim (\Delta/v_F)^2 T_C$. Finally, we have the following expression for Φ

$$\Phi = \frac{I^2 S m^2}{k_F^2} \frac{1}{2\pi^2} \rho \int_0^\infty \frac{x^{1/2} dx}{\exp x - 1} \frac{1}{T^*/T - x} \quad (11)$$

At the very low temperatures $T < T^*$, this result is in agreement with the qualitative considerations presented above:

$$\Phi = \frac{S - \langle S^z \rangle}{2S} \rho \propto \left(\frac{T}{T_C} \right)^{3/2} \rho \quad (12)$$

Nevertheless, for $T > T^*$ we have absolutely different temperature dependence of the spin polarization:

$$\Phi = 1.29 \frac{(q^*)^3}{4S\pi^2} \left(\frac{T}{T^*} \right)^{1/2} \rho \quad (13)$$

This conclusion is rather important since the crossover temperature T^* can be small and a simple estimation (8) may be valid only for very low temperatures. Moreover, it turns out that the temperature dependence of the polarization at $T > T^*$ is not universal at all. Note that the model of rigid spin splitting used above is not applicable for real HMF where the gap has hybridization origin [1, 2], in contrast to the case of degenerate ferromagnetic semiconductors. The simplest model for the HMF consists of a “normal” metallic spectrum for the majority electrons and a hybridization gap for the minority ones ($\xi_{\mathbf{k}} \equiv t_{\mathbf{k}\uparrow} - E_F$)

$$t_{\mathbf{k}\uparrow} - E_F = \frac{k^2 - k_F^2}{2m}, \quad t_{\mathbf{k}\downarrow} - E_F = \frac{1}{2} \left(\xi_{\mathbf{k}} + \text{sgn}(\xi_{\mathbf{k}}) \sqrt{\xi_{\mathbf{k}}^2 + \Delta^2} \right), \quad (14)$$

where we assume for simplicity that the Fermi energy lies exactly in the middle of the hybridization gap. Otherwise one needs to shift $\xi_{\mathbf{k}} \rightarrow \xi_{\mathbf{k}} + E_0 - E_F$ in the last equation, E_0 being the middle of the gap. Further, in the expression for $t_{\mathbf{k}+\mathbf{q}\downarrow}$ one can replace $\xi_{\mathbf{k}+\mathbf{q}}$ by $\mathbf{v}_{\mathbf{k}}\mathbf{q}$, $\mathbf{v}_{\mathbf{k}} = \mathbf{k}/m$, and use the fact that $\xi_{\mathbf{k}} = 0$ owing to the delta-function in the definition of Φ . Since a small q give the main contribution to the estimated integral, we can assume $I_{\mathbf{k},\mathbf{k}+\mathbf{q}} \simeq I_{\mathbf{k},\mathbf{k}}$. Then one has the following expression

$$\Phi = 2S \sum_{\mathbf{k}\mathbf{q}} I_{\mathbf{k},\mathbf{k}}^2 N_{\mathbf{q}} \delta(\xi_{\mathbf{k}}) A_{\mathbf{k}\mathbf{q}}, \quad A_{\mathbf{k}\mathbf{q}} = -\frac{\partial}{\partial \omega_{\mathbf{q}}} \left\langle \frac{1}{t_{\mathbf{k}+\mathbf{q}\downarrow} - t_{\mathbf{k}\uparrow} - \omega_{\mathbf{q}}} \right\rangle \Big|_{\omega_{\mathbf{q}}=0} \quad (15)$$

where the angular brackets means the average over angles of the vector \mathbf{k} . Simple calculations gives the final result:

$$A_{\mathbf{k}\mathbf{q}} = \frac{8}{v_F q \Delta} \left(\frac{2}{3} \left[X^3 - (X^2 + 1)^{3/2} + 1 \right] + X \right), \quad (16)$$

where $X = k_F q / m \Delta \equiv q/q^*$ (q^* is linear in Δ). At $X \gg 1$ corresponding to $T \gg T^* = Dq^{*2}$, one has, instead of Eq.(13), the following estimation

$$\Phi = \sum_{\mathbf{k}\mathbf{q}} 2I^2 S N_{\mathbf{q}} \delta(\xi_{\mathbf{k}}) \frac{16}{3v_F q \Delta} \propto q^* \sum_{\mathbf{q}} \frac{N_{\mathbf{q}}}{q} \propto \frac{T^{*1/2}}{T_C^{1/2}} T \ln \frac{T}{T^*} \quad (17)$$

At $X \ll 1$ ($T \ll T^*$) we get an universal $T^{3/2}$ behavior

$$\Phi = \rho \sum_{\mathbf{q}} N_{\mathbf{q}} \propto \frac{T^{3/2}}{T_C^{1/2}} \quad (18)$$

The density of NQP states is zero at the Fermi energy only for $T = 0$, while for finite temperatures it is proportional to the following integral

$$N(E_F) \propto \int_0^\infty d\omega \frac{\overline{K}(\omega)}{\sinh(\omega/T)}, \quad (19)$$

where $\overline{K}(\omega)$ is a spectral density of the spin fluctuations [24, 10, 12]. Generally speaking, for temperatures which are comparable with the Curie temperature T_C there are no essential difference between the half-metallic and “ordinary” ferromagnets since a gap of the HMF is filled. Corresponding analysis for a model of conduction electrons interacting with “pseudospin” excitations in “ferroelectric” semiconductors is performed in Ref. [12]. Symmetrical part of the $N(E)$ with respect to the E_F in the gap can be attributed to the smearing of electronic states by the electron-magnon scattering, while asymmetrical one is the density of NQP states due to the Fermi distribution function. Note that this filling of the gap is very important for possible applications of the HMF in spintronics: they really have some advantages only in the region of $T \ll T_C$. Since a single-particle Stoner-like theory leads to much less restrictive, but unfortunately completely wrong condition $T \ll \Delta$, a many-body treatment of the HMF problem is inevitable.

3 First-principle calculations of nonquasiparticle states: a dynamical mean field theory

A history of the HMF starts from the band-structure of semi Heusler alloy NiMnSb [1]. Later numerous first-principle electronic structure investigations of the HMF have been carried out (see, e.g., recent papers [27, 28, 29, 30] and a review of early works in Ref. [2]). All of them are based on a standard local density approximation (LDA) or generalized gradient approximation (GGA) to the density functional theory, and, sometimes, on the LDA+U approximation (see Ref. [31] for CrO₂). Of course, essential correlation effects such as NQP states cannot be considered in these techniques.

Recently, a successful approach has been proposed [32, 33] to include correlation effects into the first-principle electronic structure calculations by combining the LDA scheme with the dynamical mean-field theory (DMFT). The DMFT maps a lattice many-body system onto quantum impurity models subject to a self-consistent condition (for a review, see Ref.[34]). In this way, the complex lattice many-body problem splits into simple one-body crystal problem with a local self-energy and the effective many-body impurity problem. In a sense, the approach is complementary to the local density approximation [35, 36, 37] where the many-body problem splits into one-body problem for a crystal and many-body problem for *homogeneous* electron gas. Naively speaking, the LDA+DMFT method [32, 33] treats localized *d*- and *f*-electrons in spirit of the DMFT and delocalized *s*, *p*-electrons in spirit of the LDA. Due to numerical and analytical techniques developed for solution the effective quantum-impurity problem [34], the DMFT become a very efficient and extensively used approximation for local energy dependent self-energy $\Sigma(\omega)$. The accurate LDA+DMFT scheme can be used for calculating a large number of systems with different strength of electron correlations (for detailed description of the method and computational results, see Refs.

[38, 39, 40]). Following the recent work [16] we present here first LDA+DMFT results for the electronic structure calculations of a “prototype” half-metallic ferromagnet NiMnSb.

Before considering the real HMF case, it is worthwhile to check the applicability of DMFT scheme for quantitative description of the NQP states. The DMFT is considered as an *optimal* local approximation which means that the self-energy depends only on the energy and not on the quasimomentum [34]. At the same time, the NQP states are connected with the self-energy (3) which is almost local. It will be *exactly* local if we neglect magnon energies in comparison with the electron bandwidth, which is rather accurate approximation for realistic parameters. The local approximation means formally that we replace the \mathbf{q} -dependent magnon spectral density by the average one, as in the Eq.(19). Such a procedure has been analyzed and justified in the Ref. [41]. It should be stressed that an accurate description of the *magnon* spectrum is not important for existence of the NQP states as well as for proper estimation of their spectral weight, but can be important for an explicit shape of the DOS tail in the vicinity of the Fermi level (see Eq.(6)).

Let us start from the DMFT calculations for the one-band Hubbard Hamiltonian

$$H = - \sum_{i,j,\sigma} t_{ij} (c_{i\sigma}^\dagger c_{j\sigma} + c_{j\sigma}^\dagger c_{i\sigma}) + U \sum_i n_{i\uparrow} n_{i\downarrow}, \quad (20)$$

on the Bethe lattice with coordination $z \rightarrow \infty$ and nearest-neighbor hopping $t_{ij} = t/\sqrt{z}$ (in this limit the DMFT is formally exact [34]). In this case the DOS have a semicircular form:

$$N(\epsilon) = \frac{1}{2\pi t^2} \sqrt{4t^2 - \epsilon^2} \quad (21)$$

In order to stabilize the HMF state in our toy model, we have added an external magnetic spin splitting Δ , which mimics the local Hund polarization from other electrons in the real NiMnSb compound. This HMF state corresponds to a mean-field (Hartree-Fock) solution with a LSDA-like DOS (Fig. (4)).

We can study an average magnon spectrum in this model through the two-particle correlation function. The local spin-flip susceptibility

$$\chi_{loc}^{+-}(\tau) = \langle S^+(\tau) S^-(0) \rangle = \langle c_\uparrow^\dagger(\tau) c_\downarrow(\tau) c_\downarrow^\dagger(0) c_\uparrow(0) \rangle, \quad (22)$$

represents the response function required. We have calculated this function using the numerically exact QMC procedure [42].

The model DMFT results are presented in Fig. 4. In comparison with a simple Hartree-Fock solution (dashed line) one can see an additional well-pronounced states appearing in the spin-down gap region, just above the Fermi level. This new many-body feature corresponds to the NQP states. In addition to these states visible in both spin channels of the DOS around 0.5 eV, a many-body satellite appears at the energy of 3.5 eV.

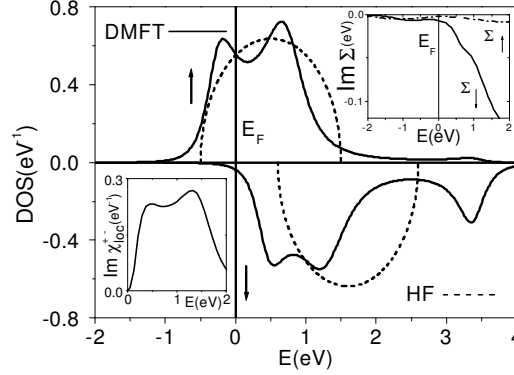


Fig. 4. Density of states for HMF in the Hartree-Fock (HF) approximation (dashed line) and the QMC solution of DMFT problem for semi-circular model (solid line) with the band-width $W = 2$ eV, Coulomb interaction $U = 2$ eV, spin-splitting $\Delta = 0.5$ eV, chemical potential $\mu = -1.5$ eV and temperature $T = 0.25$ eV. Insets: imaginary part of the local spin-flip susceptibility (left) and the spin-resolved selfenergy (right).

The left inset in the Fig. 4 represents the imaginary part of local spin-flip susceptibility. One can see a well pronounced shoulder (around 0.5 eV), which is connected with an average magnon DOS. In addition there is a broad maximum (at 1 eV) corresponding to the Stoner excitation energy. The right inset in the Fig. 4 represents the imaginary part of self-energy calculated from our “toy model”. The spin up channel can be described by a Fermi-liquid type behavior with a parabolic energy dependence $-\text{Im}\Sigma^\uparrow \propto (E - E_F)^2$, whereas in the spin down channel the imaginary part $-\text{Im}\Sigma^\downarrow$ shows the 0.5 eV nonquasiparticle shoulder. Due to the relatively high temperature of our QMC calculation (an exact enumeration, technique with the number of time-slices equal to $L = 24$) the NQP tail goes a bit below the Fermi level, in agreement with Eq.(19); at temperature $T = 0$ the NQP tail should end exactly at the Fermi level.

Let us move to the calculations for real material - NiMnSb. The details of computational scheme have been described in the Ref. [16], and only the key points will be mentioned here. In order to integrate the DMFT approach into the band structure calculation the so called exact muffin-tin orbital method (EMTO) [43, 44] was used. In the EMTO approach, the effective one-electron potential is represented by the optimized overlapping muffin-tin potential, which is the best possible spherical approximation to the full one-electron potential. The implementation of the DMFT scheme in the EMTO method is described in detail in the Ref. [45]. One should note that in addition to the usual self-consistency of the many-body problem (self-consistency of the self-energy), a charge self-consistency has been achieved [40].

For the interaction Hamiltonian, a most general rotationally invariant form of the generalized Hubbard Hamiltonian has been used [33]. The effective many-body impurity problem is solved using the spin polarized T -matrix plus fluctuation-exchange approximation (a so-called SPTF) scheme proposed in the Ref. [46], which is a development of the earlier approach [33]. The SPTF approximation is a multiband spin-polarized generalization of a well-known fluctuation exchange (FLEX) approximation [47], but with a different treatment of the particle-hole (PH) and particle-particle (PP) channels. The particle-particle (PP) channel is described by a T -matrix approach [48] yielding a renormalization of the effective interaction. The static part of this effective interaction is used explicitly in the particle-hole channel.

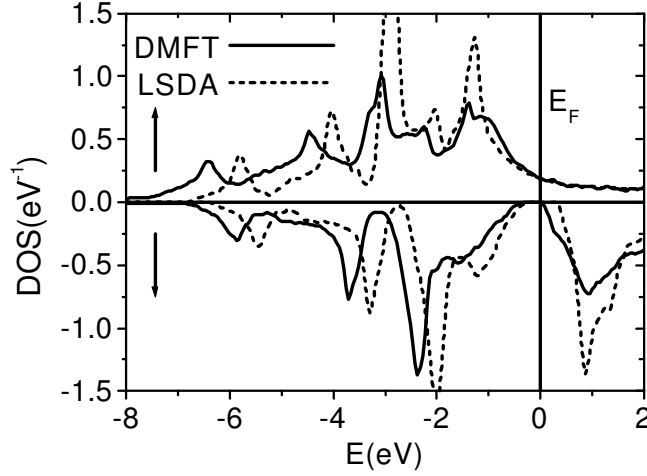


Fig. 5. Density of states for HfM NiMnSb in LSDA scheme (dashed line) and in LDA+DMFT scheme (solid line) with effective Coulomb interaction $U=3$ eV, exchange parameter $J=0.9$ eV and temperature $T=300$ K. The nonquasiparticle state is evidenced just above the Fermi level.

There are various methods to estimate the required values of the on-site Coulomb repulsion energy U and exchange interaction energy J for realistic materials. The constrained LDA calculation [49] estimates an average Coulomb interaction between the Mn d electrons as $U = 4.8$ eV with an exchange interaction energy of $J = 0.9$ eV. However, this method is adequate for a typical insulating screening and in general is not accurate for a metallic kind of screening. The latter will lead to a smaller value of U . Unfortunately, there are no reliable schemes to calculate U for metals, therefore the results for different values of U in the energy interval from 0.5 eV to the constrained LDA value $U = 4.8$ eV have been tested. At the same time, the results of

constrained LDA calculations for the Hund exchange parameter J do not depend on metallic screening and should be reliable enough. It appeared that the LDA+DMFT results are not very sensitive to the value of U , due to the T -matrix renormalization. Fig. 5 represents the results for DOS using LSDA and LDA+DMFT (with $U = 3$ eV and $J = 0.9$ eV) approaches.

It is important to mention that the magnetic moment per formula unit is not sensitive to the U values and is equal exactly $\mu = 4 \mu_B$, which suggests that the half-metallic state is stable with respect to the introduction of the correlation effects. In addition, the DMFT gap in the spin down channel, defined as the distance between the occupied part and the starting point of nonquasiparticle state's "tail", is also not very sensitive to the U values. For different U 's a slope of the "tail" is slightly changed, but the total DOS is weakly U -dependent due to the same T -matrix renormalization effects.

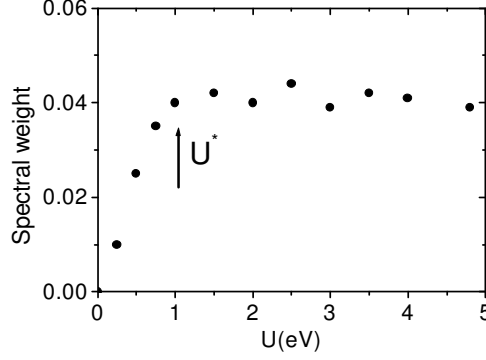


Fig. 6. Spectral weight of the nonquasiparticle state, calculated as function of average on-site Coulomb repulsion U at temperature $T=300$ K.

Thus the correlation effects do not effect too strongly a general feature of the electron energy spectrum (except for smearing of DOS which is due to the finite temperature $T = 300$ K in our calculations). The only qualitatively new effect is the appearance of a "tail" of the NQP states in the energy gap above the Fermi energy. Their spectral weight for realistic values of the parameters is not very small, which means that the NQP should be well pronounced in the corresponding experimental data. A relatively weak dependence of the NQP spectral weight on the U value (Fig. 6) is also a consequence of the T -matrix renormalization [46]. One can see that the T -matrix depends slightly on U provided that the latter is larger than the widths of the main DOS peaks near the Fermi level in an energy range of 2 eV (this is of the order of $U^* \simeq 1$ eV).

For the spin-up states we have a normal Fermi-liquid behavior $-\text{Im}\Sigma_d^\uparrow(E) \propto (E - E_F)^2$ with a typical energy scale of the order of several eV. The spin-

down self-energy behaves in a similar way below the Fermi energy, with a slightly smaller energy scale (which is still larger than 1 eV). At the same time, a significant increase in $\text{Im}\Sigma_d^\downarrow(E)$ with a much smaller energy scale (few tenths of eV) occurs just above the Fermi level, which is more pronounced for t_{2g} states (Fig. 7). The similar behavior of the imaginary part of electronic self-energy and the DOS just above Fermi level is a signature of the NQP states and is also noticed in the model calculation (Fig. 4).

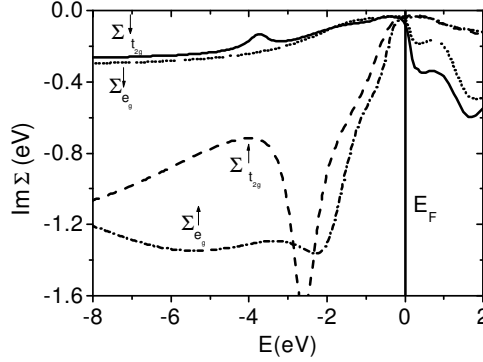


Fig. 7. The imaginary part of self-energies $\text{Im}\Sigma_d^\downarrow$ for t_{2g} (solid line) and e_g (dotted line), $\text{Im}\Sigma_d^\uparrow$ for t_{2g} (dashed line) and e_g (dashed dotted line) respectively.

Thus the main results of the Ref. [16] are (i) the existence of the NQP states in real electronic structure of a specific compound, and (ii) estimation of their spectral weight in the LDA+DMFT approach. The temperature dependence of the NQP density of states in the gap, which is important for possible applications of the HMF in spintronics, can be analyzed in the present technique.

4 X-ray absorption and emission spectra. Resonant x-ray scattering

Now we discuss the manifestations of NQP states in the core level spectroscopy [50]. Various spectroscopy techniques such as x-ray absorption, x-ray emission, and photoelectron spectroscopies (xas, xes, and xps) give an important information about the electronic structure of the HMF and related compounds, such as ferromagnetic semiconductors and colossal magnetoresistance materials (see, e.g., Refs. [51, 52, 53, 54]). It is well known that the many-body effects, particularly dynamical core hole screening, may be important for a core level spectroscopy even in the case that a system is not strongly correlated in the initial state [55, 56]. Therefore it is very interesting

to look on the interplay of these effects with the NQP states, which are of essentially many-body origin themselves.

To consider a core level problem in the HMF we use the same Hamiltonian of the $s-d$ exchange model, Eq. (1) in the presence of the external potential U induced by the core hole:

$$\mathcal{H}' = \varepsilon_0 f^\dagger f - U \sum_{\mathbf{k}\mathbf{k}'\sigma} c_{\mathbf{k}\sigma}^\dagger c_{\mathbf{k}'\sigma} f^\dagger f, \quad (23)$$

where f^\dagger, f are core hole operators. It is useful to write down the equation of motion for the retarded two-particle Green's function [57]

$$G_{\mathbf{k}\mathbf{k}'}^\sigma(E) = \langle\langle c_{\mathbf{k}\sigma} f | f^\dagger c_{\mathbf{k}'\sigma}^\dagger \rangle\rangle_E, \quad (24)$$

which determines x-ray absorption and emission spectra [55]. Using a magnon representation for the spin operators, we derive the following equation for two-particle Green's function:

$$(E - t_{\mathbf{k}\sigma}) G_{\mathbf{k}\mathbf{k}'}^\sigma(E) = (1 - n_f - n_{\mathbf{k}}^\sigma) \left[\delta_{\mathbf{k}\mathbf{k}'} - U \sum_{\mathbf{p}} G_{\mathbf{p}\mathbf{k}'}^\sigma(E) \right] - I \sum_{\mathbf{r}} F_{\mathbf{k}-\mathbf{r},\mathbf{r},\mathbf{k}'}^\sigma(E) \quad (25)$$

where n_f is the occupation number for the f -hole in the initial state, which is further on will be put to zero and E is the electron energy with respect to ε_0). We will take into account the occupation numbers $n_{\mathbf{k}}^\sigma$ in a simple ladder approximation which works well in the limit of small concentrations of mobile carriers, except for the immediate vicinity of the Fermi edge. Here, we do not treat the problem of the x-ray edge singularity where more advanced approaches are necessary [55, 56]. The following notation has been used in Eq.(25):

$$F_{\mathbf{k}-\mathbf{p},\mathbf{q},\mathbf{k}'}^\sigma(E) = (2S)^{1/2} \langle\langle b_{\mathbf{q}}^\sigma c_{\mathbf{k}-\mathbf{p},-\sigma} f | f^\dagger c_{\mathbf{k}'\sigma}^\dagger \rangle\rangle_E, \quad (26)$$

where $b_{\mathbf{q}}^+ = b_{-\mathbf{q}}^\dagger$, $b_{\mathbf{q}}^- = b_{\mathbf{q}}$ are the Holstein-Primakoff magnon operators [18]. The Green's function F satisfies the equation

$$\begin{aligned} (E - t_{\mathbf{k}-\mathbf{p},-\sigma} + \sigma\omega_{\mathbf{q}}) F_{\mathbf{k}-\mathbf{p},\mathbf{q},\mathbf{k}'}^\sigma(E) &= -U(1 - n_{\mathbf{k}-\mathbf{p}}^{-\sigma}) \Psi_{\mathbf{q},\mathbf{k}'}^\sigma(E) \\ -I(N_{\mathbf{q}}^\sigma + \sigma n_{\mathbf{k}-\mathbf{p}}^{-\sigma}) [2S G_{\mathbf{k}-\mathbf{p}+\mathbf{q},\mathbf{k}'}^\sigma(E) + \sigma \sum_{\mathbf{r}} F_{\mathbf{k}-\mathbf{p}+\mathbf{q}-\mathbf{r},\mathbf{r},\mathbf{k}'}^\sigma(E)], \end{aligned} \quad (27)$$

where we have performed decouplings in the spirit of ladder approximation, $\langle b_{-\mathbf{q}}^\sigma b_{\mathbf{q}}^{-\sigma} \rangle = N_{\mathbf{q}}^\sigma = \sigma N(\sigma\omega_{\mathbf{q}})$, $N(\omega)$ is the Bose function, and Ψ is defined as

$$\Psi_{\mathbf{q},\mathbf{k}'}^\sigma(E) = \sum_{\mathbf{r}} F_{\mathbf{k}-\mathbf{r},\mathbf{q},\mathbf{k}'}^\sigma(E) \quad (28)$$

For $U = 0$ we have $G_{\mathbf{k}\mathbf{k}'}^\sigma(E) = (1 - n_{\mathbf{k}}^\sigma) \delta_{\mathbf{k}\mathbf{k}'} G_{\mathbf{k}}^\sigma(E)$, where $G_{\mathbf{k}}^\sigma(E)$ is the one-electron Green's function of the ideal crystal (cf. Eq.(3)),

$$G_{\mathbf{k}}^{\sigma}(E) = [E - t_{\mathbf{k}\sigma} - \Sigma_{\mathbf{k}\sigma}(E)]^{-1}, \quad \Sigma_{\mathbf{k}\sigma}(E) = \frac{2\bar{S}I^2Q_{\mathbf{k}}^{\sigma}}{1 + \sigma IQ_{\mathbf{k}}^{\sigma}} \quad (29)$$

Note that the Eq. (29) gives correctly the exact Green's function in the limit of an empty conduction band at $T = 0$ [58, 59, 10].

In a general case, we have the three-particle problem (conduction electron, core hole and magnon) which requires a careful mathematical investigation. However, we can use the facts that the magnon frequencies are much smaller than typical electron energies and energy resolution of xas and xes methods. Neglecting spin dynamics, the equations (25), (27) can be solved exactly in a rather simple way for the case of zero temperatures ($N_{\mathbf{q}}^{+} = 0$, $N_{\mathbf{q}}^{-} = 1$). Under these conditions, Q does not depend on quasimomenta, and $\Psi_{\mathbf{q},\mathbf{k}'}^{\sigma}$ does not depend on \mathbf{q} , since the electron and magnon operator should belong to the same perturbed site:

$$\Psi_{\mathbf{q},\mathbf{k}'}^{\sigma}(E) = \Psi_{\mathbf{k}'}^{\sigma}(E) = (2S)^{1/2} \langle \langle b^{\sigma} c_{-\sigma} f | f^{\dagger} c_{\mathbf{k}'\sigma}^{\dagger} \rangle \rangle_E \quad (30)$$

We find in this case

$$\Psi_{\mathbf{k}'}^{\sigma}(E) = -\frac{2ISQ^{\sigma}(E)}{1 + UP^{-\sigma}(E) + \sigma IQ^{\sigma}(E)} R_{\mathbf{k}'}^{\sigma}(E) \quad (31)$$

$$R_{\mathbf{k}'}^{\sigma}(E) = \sum_{\mathbf{k}} G_{\mathbf{k}\mathbf{k}'}^{\sigma}(E), \quad P^{\sigma}(E) = \sum_{\mathbf{k}} \frac{1 - n_{\mathbf{k}}^{\sigma}}{E - t_{\mathbf{k}\sigma}} \quad (32)$$

After substituting Eq.(31) into Eq.(25) we obtain the following equation for the Green's function G

$$[E - t_{\mathbf{k}\sigma} - \Sigma^{\sigma}(E)] G_{\mathbf{k}\mathbf{k}'}^{\sigma}(E) = \delta_{\mathbf{k}\mathbf{k}'} - U_{ef}^{\sigma}(E) \sum_{\mathbf{p}} G_{\mathbf{p}\mathbf{k}'}^{\sigma}(E) \quad (33)$$

with the renormalized core hole potential:

$$U_{ef}^{\sigma}(E) = U \left[1 + \frac{\Sigma^{\sigma}(E)P^{-\sigma}(E)}{1 + UP^{-\sigma}(E) + \sigma IQ^{\sigma}(E)} \right]. \quad (34)$$

Here we neglect the factor $(1 - n_{\mathbf{k}}^{\sigma})$, since the band filling is small. Therefore one has a standard result for the impurity scattering with renormalized energy spectrum $E_{\mathbf{k}\sigma} = t_{\mathbf{k}\sigma} + \Sigma^{\sigma}(E)$ and the effective impurity potential $U_{ef}^{\sigma}(E)$. A local DOS is given by the following expression:

$$N_{\text{loc}}^{\sigma}(E) = -\frac{1}{\pi} \text{Im} G_{00}^{\sigma}(E) \quad (35)$$

with

$$G_{00}^{\sigma}(E) = \sum_{\mathbf{k}\mathbf{k}'} G_{\mathbf{k}\mathbf{k}'}^{\sigma}(E) = \frac{R_{\sigma}(E)}{1 + U_{ef}^{\sigma}(E)R_{\sigma}(E)} \quad (36)$$

where $R_{\sigma}(E) = \sum_{\mathbf{k}} G_{\mathbf{k}}^{\sigma}(E)$, and $G_{\mathbf{k}}^{\sigma}(E)$ is given by Eq.(29).

Generally speaking, theoretical investigation of the core level spectra requires numerical calculations of realistic band structure. We restrict ourselves to simple model calculations for the bare semicircular DOS from the Eq.(21).

The local Green function from Eq. (35) describes the absorption spectrum for $E > E_F$ and emission spectrum for $E < E_F$. As follows from the Eq. (35), (36), the experimental spectra is given by somewhat different expression than the DOS in an initial state, and new effects can occur.

For $I > 0$ the results of Eq.(34)-(36) provide full solution of the Kondo problem for an impurity in the ferromagnet, within the parquet approximation [60]. In the case of $I < 0$, the situation is complicated by the presence of the “false” Kondo divergence in the T -matrix [61]. However, this difficulty is not important for the x-ray problem where a large damping is always present, and experiments are performed at sufficiently high temperatures with rather poor resolution compared to a scale of the “Kondo temperature”. To a leading order in U and I we obtain

$$\begin{aligned} \delta N_{\text{loc}}^{\sigma}(E) = & \frac{1 - \text{Re}(U_{ef}^{\sigma}(E)/\Sigma^{\sigma}(E)) |R_{\sigma}^2(E)/R'_{\sigma}(E)|}{\left|1 + U_{ef}^{\sigma}(E)R_{\sigma}(E)\right|^2} \delta N^{\sigma}(E) \\ & - \frac{\text{Re}(U_{ef}^{\sigma}(E)/P^{-\sigma}(E)) |R_{\sigma}(E)|^2}{\left|1 + U_{ef}^{\sigma}(E)R_{\sigma}(E)\right|^2} \frac{1}{\pi} \text{Im}P^{-\sigma}(E) \end{aligned} \quad (37)$$

The term in Eq.(37) with $\text{Im}P^{-\sigma}(E)$ has a smooth contribution to the spectrum. In particular, it is non-zero in the energy gap. Note that for the emission spectra such term is absent. The NQP contributions to the absorption (for $I > 0$) and emission spectra (for $I < 0$) are proportional to $\delta N^{\sigma}(E)$.

One can see from Fig.(8) that the upturn of the NQP tail which occurs for $I > 0$ becomes more sharp, although the jump near E_F weakens. For $I < 0$ case, the spectral weight of NQP contributions also increases in the presence of the core hole (see Fig.(9)). These effects have a simple physical interpretation. Since $U_{ef}^{\sigma}(E) > 0$ and for small band filling $R_{\sigma}(E) < 0$ near E_F , the denominator of the expression (37) gives a considerable enhancement of the NQP contributions to the spectra in comparison with those to the DOS. However, effects of interaction U turn out to be non-trivial and do not reduce to a constant factor in the self-energy. Strong interaction with the core hole results in a deformation of conduction band. With increasing U the spectral density concentrated at bottom of the band. This effect is very important for the NQP states located in this region. Therefore the spectral weight of the NQP states increases. At very large, probably unrealistic values of U , a bound state is formed near the band bottom, and the NQP spectral weight becomes suppressed owing to factor of U in the denominator of Eq.(34).

To probe a “spin-polaron” nature of the NQP states more explicitly, it would be desirable to use spin-resolved spectroscopical methods such as x-ray magnetic circular dichroism (XMCD, for a review see Ref. [62]). Owing to

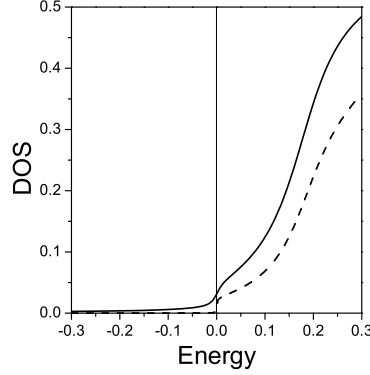


Fig. 8. The local density of states $N_{\text{loc}}^{\downarrow}(E)$ (solid line) for a half-metallic ferromagnet with $S = 1/2, I = 0.3$ in the presence of the core hole potential $U = 0.2$; smearing $E + i\delta$ is introduced with $\delta = 0.01$. The dashed line shows the DOS $N_{\downarrow}(E)$ for the ideal crystal with spin dynamics being neglected. The value of E_F calculated from the band bottom is 0.15. The energy E is referred to the Fermi level.

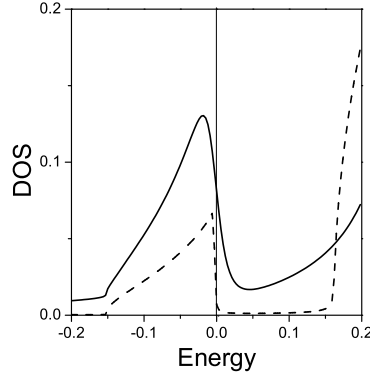


Fig. 9. The local density of states $N_{\text{loc}}^{\uparrow}(E)$ (solid line) for a half-metallic ferromagnet with $S = 1/2, I = -0.3, \delta = 0.025$ in the presence of the core hole potential $U = 0.2$. The dashed line shows the DOS $N_{\uparrow}(E)$ for the ideal crystal. The value of E_F calculated from the band bottom is 0.15.

interference of electron-magnon scattering and “exciton” effects from interaction of electrons with the core hole, the NQP contributions to x-ray spectra can be considerably enhanced in comparison with those to the DOS of ideal crystal.

Now we consider the NQP effects in resonant x-ray scattering processes. It was observed recently that the elastic peak of the x-ray scattering in CrO_2 is more pronounced than in usual Cr compounds [53]. The authors of this work have put forward some qualitative arguments that the NQP states may give larger contributions to resonant x-ray scattering than usual itinerant

electron states. Here we shall treat this problem quantitatively and estimate explicitly the corresponding enhancement factor. The intensity of resonant x-ray emission induced by the photon with the energy ω and polarization q is given by the Kramers-Heisenberg formula [63, 52, 64]

$$I_{q'q}(\omega', \omega) \propto \sum_n \left| \sum_l \frac{\langle n | C_{q'} | l \rangle \langle l | C_q | 0 \rangle}{E_0 + \omega' - E_l - i\Gamma_l} \right|^2 \delta(E_n + \omega' - E_0 - \omega), \quad (38)$$

here q', ω' are the polarization and energy of the emitted photon, $|n\rangle$, $|0\rangle$ and $|l\rangle$ are the final, initial and intermediate states of the scattering system with the energies E_i , respectively, and C_q is the operator of a dipole moment for the transition, which is proportional to $(fc + c^\dagger f^\dagger)$. For simplicity we assume hereafter that Γ_l does not depend on the intermediate state: $\Gamma_l = \Gamma$, and take into account only the main x-ray scattering channel where the hole is filled by conduction electron. Assuming that the electron-photon interaction that induces the transition is contact, the expression for threshold scattering intensity has following form [65]

$$I_{\omega'} \propto \sum_{\sigma\sigma'} \int_0^\infty dt_1 \int_0^\infty dt_2 \exp[-i(\omega' - \varepsilon_0)(t_1 - t_2) - \Gamma(t_1 + t_2)] \\ \langle 0 | c_\sigma \exp(i\mathcal{H}_f t_1) c_{\sigma'}^\dagger \exp[i\mathcal{H}_i(t_2 - t_1)] c_{\sigma'} \exp(-i\mathcal{H}_f t_2) c_\sigma^\dagger | 0 \rangle, \quad (39)$$

where H_f and H_i are conduction-electron Hamiltonians with and without core hole, respectively. The complicated correlation function in Eq.(39) can be decoupled in the ladder approximation which is exact for the empty conduction band. Then one can obtain [65]

$$I_{\omega'} \propto \left| \sum_\sigma G_{00}^\sigma(z) \right|^2, \quad (40)$$

where $z = \omega' - E_0 + i\Gamma$. Owing to a jump in the DOS at the Fermi level, the NQP part of the Green's function contains a large logarithm $\ln(W/z)$ at small z , W being a bandwidth. It means that the corresponding contribution to the elastic x-ray scattering intensity ($\omega' = E_0$) is enhanced by a factor of $\ln^2(W/\Gamma)$, which makes a quantitative estimation for the qualitative effect discussed in Ref. [53]. Of course, the smearing of the jump in the density of NQP states by spin dynamics is irrelevant provided that $\Gamma > \overline{\omega}$, where $\overline{\omega}$ is a characteristic magnon frequency.

5 Transport properties

Transport properties of the HMF are a subject of numerous experimental investigations (see, e.g., recent works on CrO₂ [66], NiMnSb [67], and the

reviews [2, 68, 69]). At the same time, a theoretical interpretation of these results is still problematic. Concerning electronic scattering mechanisms, the most important difference between the HMF and “standard” itinerant electron ferromagnets like iron or nickel is the absence of one-magnon scattering processes in the former case [2]. Two-magnon scattering processes have been considered many years ago for both the broad-band case (a weak s - d exchange interaction) [70] and narrow-band case (a “double exchange model”) [71]. Obtained temperature dependence of resistivity have the form $T^{7/2}$ and $T^{9/2}$, respectively. At low enough temperatures the first result fails and should be replaced by $T^{9/2}$ as well [72]; the reason is a compensation of transverse and longitudinal contributions in the long-wavelength limit, which is a consequence of the rotational symmetry of the s - d exchange Hamiltonian [73, 74]. Recently a general interpolation theory has been formulated [75]. Here we discuss main results of this work with a special emphasize to the NQP effects.

In the spin-wave region the Hamiltonian (1) can be rewritten in the form

$$\begin{aligned} \mathcal{H} = \mathcal{H}_0 - I(2S)^{1/2} \sum_{\mathbf{k}\mathbf{q}} (c_{\mathbf{k}\uparrow}^\dagger c_{\mathbf{k}+\mathbf{q}\downarrow} b_{\mathbf{q}}^\dagger + h.c.) \\ + I \sum_{\mathbf{k}\mathbf{q}\mathbf{p}\sigma} \sigma c_{\mathbf{k}\sigma}^\dagger c_{\mathbf{k}+\mathbf{q}-\mathbf{p}\sigma} b_{\mathbf{q}}^\dagger b_{\mathbf{p}} \end{aligned} \quad (41)$$

Here the zero-order Hamiltonian includes non-interacting electrons and magnons:

$$\mathcal{H}_0 = \sum_{\mathbf{k}\sigma} t_{\mathbf{k}\sigma} c_{\mathbf{k}\sigma}^\dagger c_{\mathbf{k}\sigma} + \sum_{\mathbf{q}} \omega_{\mathbf{q}} b_{\mathbf{q}}^\dagger b_{\mathbf{q}}, \quad (42)$$

with the spin splitting $\Delta = 2IS$ being included in \mathcal{H}_0 . In the half-metallic case spin-flip processes do not appear in the second order in I , since the states with only one spin projection presented at the Fermi level. At the same time, we have to consider the renormalization of the longitudinal processes in higher orders in I (formally, we need to include all terms up to the second order in a quasiclassical small parameter $1/S$). To this end we eliminate from the Hamiltonian the terms which are linear in the magnon operators by using the canonical transformation [73]. Then, the effective Hamiltonian has a following form

$$\tilde{\mathcal{H}} = \mathcal{H}_0 + \frac{1}{2} \sum_{\mathbf{k}\mathbf{q}\mathbf{p}\sigma} (\mathcal{A}_{\mathbf{k}\mathbf{q}}^\sigma + \mathcal{A}_{\mathbf{k}+\mathbf{q}-\mathbf{p},\mathbf{q}}^\sigma) c_{\mathbf{k}\sigma}^\dagger c_{\mathbf{k}+\mathbf{q}-\mathbf{p}\sigma} b_{\mathbf{q}}^\dagger b_{\mathbf{p}}, \quad (43)$$

where

$$\mathcal{A}_{\mathbf{k}\mathbf{q}}^\sigma = \sigma I \frac{t_{\mathbf{k}+\mathbf{q}} - t_{\mathbf{k}}}{t_{\mathbf{k}+\mathbf{q}} - t_{\mathbf{k}} + \sigma \Delta} \quad (44)$$

is the s - d scattering amplitude, which vanishes at $q \rightarrow 0$ and thereby takes properly into account the rotational symmetry of electron-magnon interaction. More general interpolation expression for the effective amplitude which does not assume the smallness of $|I|$ or $1/S$ was obtained in Ref. [74] within

a variational approach, but it does not differ qualitatively from simple expression (44). In the case of real itinerant magnets including the HMF, a \mathbf{k} -dependence of s - d exchange parameter should be taken into account, similarly to the temperature dependence of spin polarization. However, here we restrict ourselves only to the rigid spin splitting model appropriate for degenerate ferromagnetic semiconductors. One can expect from phenomenological symmetry considerations that the temperature dependences of transport properties are rather universal.

The most general scheme for calculating the transport relaxation time is the Kubo formalism for the conductivity σ_{xx} [76]

$$\sigma_{xx} = \beta \int_0^\beta d\lambda \int_0^\infty dt \exp(-\varepsilon t) \langle j_x(t + i\lambda) j_x \rangle \quad (45)$$

where $\beta = 1/T$, $\varepsilon \rightarrow 0$, $\mathbf{j} = -e \sum_{\mathbf{k}\sigma} \mathbf{v}_{\mathbf{k}\sigma} c_{\mathbf{k}\sigma}^\dagger c_{\mathbf{k}\sigma}$ is the current operator, $\mathbf{v}_{\mathbf{k}\sigma} = \partial t_{\mathbf{k}\sigma} / \partial \mathbf{k}$ is the electron velocity. Rewriting the total Hamiltonian in the form $\mathcal{H} = \mathcal{H}_0 + \mathcal{H}_1$, the correlator in (45) may be expanded in the perturbation \mathcal{H}_1 [77]. In the second order we obtain for the electrical resistivity the following expression

$$\rho_{xx} = \sigma_{xx}^{-1} = \frac{T}{\langle j_x^2 \rangle^2} \int_0^\infty dt \langle [j_x, \mathcal{H}_1(t)] [\mathcal{H}_1, j_x] \rangle, \quad (46)$$

where $\mathcal{H}_1(t)$ is calculated with the Hamiltonian \mathcal{H}_0 . In the HMF situation the band states with one spin projection only, $\sigma = \alpha = \text{sign} I$, are present at the Fermi level. Below we consider the case $I > 0$, $\sigma = +$ and omit the spin indices in the electron spectrum. Then one can find an expression for the transport relaxation time τ defined as $\sigma_{xx} = e^2 \langle (v^x)^2 \rangle \tau$

$$\begin{aligned} \frac{1}{\tau} = & \frac{\pi}{4T} \sum_{\mathbf{k}\mathbf{k}'\mathbf{q}} (v_{\mathbf{k}}^x - v_{\mathbf{k}'}^x)^2 (\mathcal{A}_{\mathbf{k}\mathbf{q}}^\dagger + \mathcal{A}_{\mathbf{k}',\mathbf{q}-\mathbf{k}'+\mathbf{k}}^\dagger)^2 N_{\mathbf{q}} (1 + N_{\mathbf{q}-\mathbf{k}'+\mathbf{k}}) n_{\mathbf{k}} (1 - n_{\mathbf{k}'}) \\ & \times \delta(t_{\mathbf{k}'} - t_{\mathbf{k}} - \omega_{\mathbf{q}} + \omega_{\mathbf{q}-\mathbf{k}'+\mathbf{k}}) \bigg/ \sum_{\mathbf{k}} (v_{\mathbf{k}}^x)^2 \delta(t_{\mathbf{k}}) \end{aligned} \quad (47)$$

Averaging over angles of the vector \mathbf{k} leads us to the final result $1/\tau \propto I^2 \Lambda$ with

$$\Lambda = \sum_{\mathbf{p}\mathbf{q}} f_{\mathbf{p}\mathbf{q}} \frac{\beta(\omega_{\mathbf{p}} - \omega_{\mathbf{q}}) |\mathbf{p} - \mathbf{q}|}{\exp \beta \omega_{\mathbf{p}} - \exp \beta \omega_{\mathbf{q}}} (1 + N_{\mathbf{q}}) (1 + N_{\mathbf{p}}), \quad (48)$$

where $f_{\mathbf{p}\mathbf{q}} = 1$ for $p, q \gg q_0$ and

$$f_{\mathbf{p}\mathbf{q}} = \frac{[\mathbf{p} \times \mathbf{q}]^2}{(\mathbf{p} - \mathbf{q})^2 q_0^2} \quad (p, q \ll q_0). \quad (49)$$

The wavevector q_0 determines the boundary of a region where \mathbf{q} -dependence of the amplitude become important, so that $t(\mathbf{k} + \mathbf{q}) - t(\mathbf{k}) \simeq \Delta$ at $q \simeq q_0$

and the simple perturbation theory fails. In elementary one-band model of the HMF where $E_F < \Delta$ one has $q_0 \sim \sqrt{\Delta/W}$ (where W is the conduction bandwidth, and the lattice constant is put to unity) [73]. Generally speaking, q_0 may be sufficiently small provided that the energy gap is much smaller than W , which is the case for real HMF systems.

The quantity q_0 determines a characteristic temperature and energy scale $T^* = Dq_0^2 \propto D(\Delta/W)$, where $D \propto T_C/S$ is the spin-wave stiffness defined by $\omega_{\mathbf{q} \rightarrow 0} = Dq^2$, and T_C is the Curie temperature. It is important that similar crossover temperatures appears in the temperature dependence of the spin polarization (see, e.g., Eqs.(13),(17)). This means that temperature dependences of both spin polarization and transport properties can be changed at low enough temperatures within the spin-wave temperature region.

One has to bear in mind that each power of p or q yields the $T^{1/2}$ factor for temperature dependence of resistivity. At very low temperatures $T < T^*$ small quasimomenta $p, q < q_0$ gives a main contribution to the integrals. Then the temperature dependence of resistivity is equal to $\rho(T) \propto (T/T_C)^{9/2}$. Such a dependence was obtained in the large- $|I|$ case where the scale T^* is absent [71], and within a diagram approach in the broad-band case [72]. At the same time, for $T > T^*$ the function $f_{\mathbf{p}\mathbf{q}}$ in Eq. (48) can be replaced by unity, leading to $\rho(T) \propto (T/T_C)^{7/2}$, in agreement with the old results [70].

According to calculations presented here, the NQP states do *not* contribute to the temperature dependence of the resistivity for pure HMF. An opposite conclusion was made by Furukawa [78] and related to an anomalous T^3 dependence in the resistivity. However, this calculation was not based on a consistent use of the Kubo formula and, in our opinion, can be hardly justified.

On the contrary, *impurity* contributions to transport properties in the presence of potential scattering are determined mainly by the NQP states (it has been shown first in Ref. [12], see also Ref. [2]). To a second order in the impurity potential V we derive for the electron Green's function

$$G_{\mathbf{k}\mathbf{k}'\sigma}(E) = \delta_{\mathbf{k}\mathbf{k}'} G_{\mathbf{k}\sigma}^{(0)}(E) + G_{\mathbf{k}\sigma}^{(0)}(E) V G_{\mathbf{k}'\sigma}^{(0)}(E) [1 + V \sum_{\mathbf{p}} G_{\mathbf{p}\sigma}^{(0)}(E)], \quad (50)$$

where $G_{\mathbf{k}\sigma}^{(0)}(E)$ is the exact Green's function for the ideal crystal (see Eq.(2)). Neglecting vertex corrections and averaging over impurities, we obtain for the transport relaxation time in the following form

$$\delta\tau_{imp}^{-1}(E) = -2V^2 \text{Im} \sum_{\mathbf{p}} G_{\mathbf{p}\sigma}^{(0)}(E) \quad (51)$$

Thus the relaxation time is determined by the energy dependence of the density of states $N(E)$ for the interacting system near the Fermi level. The most nontrivial dependence comes from the nonquasiparticle states with the spin projection $\alpha = \text{sign}I$, which are present near the E_F . Close to the Fermi

level the NQP contribution follows the power law (6). Therefore, the impurity contribution to the resistivity is equal to

$$\frac{\delta\rho_{imp}(T)}{\rho^2} = -\delta\sigma_{imp}(T) \propto -V^2 \int dE \left(-\frac{\partial f(E)}{\partial E} \right) \delta N_{incoh}(E) \propto T^{3/2} \quad (52)$$

The contribution of the order of T^α with $\alpha \simeq 1.65$ (which is not too far from $3/2$) has been observed recently in the temperature dependence of the resistivity for NiMnSb [67].

To calculate the magnetoresistivity we take into account a gap in the magnon spectrum induced by magnetic field, $\omega_{\mathbf{q} \rightarrow 0} = Dq^2 + \omega_0$. For large external magnetic field H , in comparison with the anisotropy gap, ω_0 is proportional to H . At $T < T^*$ the resistivity is linear in magnetic field:

$$\rho(T, H) - \rho(T, 0) \propto -\omega_0 T^{7/2} / T_C^{9/2} \quad (53)$$

The situation at $T > T^*$ is more interesting since the quantity $\partial\Lambda/\partial\omega_0$ contains a logarithmic divergence with the cutoff at ω_0 or T^* . We have at $T > \omega_0, T^*$:

$$\delta\rho(T, H) \propto -\frac{T^3\omega_0}{[\max(\omega_0, T^*)]^{1/2}} \quad (54)$$

Of course, at $T < \omega_0$ the resistivity is exponentially small. A negative H -linear magnetoresistance was observed recently in CrO₂ [66]. The incoherent contribution to magnetoresistivity is given by

$$\delta\rho_{imp}(T, H) \propto \omega_0 \partial\delta N_{incoh}(\sigma T) / \partial T \propto \omega_0 \sqrt{T}. \quad (55)$$

Another useful tool to detect the NQP states is provided by tunneling phenomena [79], in particular by the Andreev reflection spectroscopy for the HMF-superconductor tunnel junction [81]. A most direct way is the measurement of a tunnel current between two pieces of the HMF with the opposite magnetization directions. To this end we consider a standard tunneling Hamiltonian (see, e.g., Ref. [55], Sect. 9.3):

$$\mathcal{H} = \mathcal{H}_L + \mathcal{H}_R + \sum_{\mathbf{k}\mathbf{p}} (T_{\mathbf{k}\mathbf{p}} c_{\mathbf{k}\uparrow}^\dagger c_{\mathbf{p}\downarrow} + h.c.), \quad (56)$$

where $\mathcal{H}_{L,R}$ are the Hamiltonians of the left (right) half-spaces, respectively, \mathbf{k} and \mathbf{p} are the corresponding quasimomenta, and spin projections are defined with respect to the magnetization direction of a given half-space (the spin is supposed to be conserving in the “global” coordinate system). Carrying out standard calculations of the tunneling current \mathcal{I} in the second order in $T_{\mathbf{k}\mathbf{p}}$ we obtain (cf. Ref. [55])

$$\mathcal{I} \propto \sum_{\mathbf{k}\mathbf{q}\mathbf{p}} |T_{\mathbf{k}\mathbf{p}}|^2 [1 + N_{\mathbf{q}} - f(t_{\mathbf{p}-\mathbf{q}})] [f(t_{\mathbf{k}}) - f(t_{\mathbf{k}} + eV)] \delta(eV + t_{\mathbf{k}} - t_{\mathbf{p}-\mathbf{q}} + \omega_{\mathbf{q}})$$

Here V is the bias voltage. For $T = 0$ one has $d\mathcal{I}/dV \propto \delta N_{incoh}(eV)$.

6 Conclusions

To conclude, we have considered the special properties of half-metallic ferromagnets which are connected with their unusual electronic structure. Further experimental investigations would be of a great importance, especially keeping in mind possible role of the HMF for different applications [2, 3, 4].

Several experiments could be performed in order to clarify the impact of the nonquasiparticle states on spintronics. Direct ways of observing the NQP states would imply the technique of Bremsstrahlung Isochromat Spectroscopy (BIS) [21] or the spin-polarized scanning tunneling microscopy (SP-STM) [15], since for the most frequent case of minority-spin gap where the NQP states lie above E_F . In contrast with the photoelectron spectroscopy of the occupied states (PES) which has to show a complete spin polarization in the HMF with minority-spin gap, the BIS spectra should demonstrate an essential depolarization of the states above the E_F . For the majority-spin-gap HMF, vice versa, the partial depolarization should be seen in the PES. The $I - V$ characteristics of half-metallic tunnel junctions for the case of antiparallel spins are completely determined by the NQP states [75, 80]. The spin-polarized STM should be able to probe these states by the differential tunneling conductivity dI/dV [55, 82]. In particular, the SP-STM with positive bias voltage can detect the opposite-spin states just above the Fermi level for surface of the HMF such as CrO_2 . The Andreev reflection spectroscopy for tunnel junction superconductor-HMF [81] can also be used in searching for experimental evidence of the NQP effects. These experimental measurements will be of crucial importance for the theory of spintronics in any tunneling devices with the HMF. Since ferromagnetic semiconductors can be considered as a special case of the HMF, an account of these states can be helpful for the proper description of spin diodes and transistors [83].

The research described was supported in part by Grant No.02-02-16443 from Russian Basic Research Foundation and by Russian Science Support Foundation.

References

1. R. A. de Groot, F. M. Mueller, P. G. van Engen, and K. H. J. Buschow, *Phys. Rev. Lett.* **50**, 2024 (1983).
2. V. Yu. Irkhin and M. I. Katsnelson, *Uspekhi Fiz. Nauk* **164**, 705 (1994) [*Phys. Usp.* **37**, 659 (1994)].
3. W. E. Pickett and J. Moodera, *Phys. Today* **54**(5), 39 (2001).
4. G. A. Prinz, *Science* **282**, 1660 (1998).
5. P. Nozieres, *Theory of Interacting Fermi Systems* (Benjamin, New York, 1964); D. Pines and P. Nozieres, *The Theory of Quantum Liquids* (Benjamin, New York, 1966).
6. S. V. Vonsovsky and M. I. Katsnelson, *Quantum Solid State Physics* (Springer, Berlin, 1989); S. V. Vonsovsky and M. I. Katsnelson, *Physica B* **159**, 61 (1989).

7. D. M. Edwards and J. A. Hertz, J. Phys. F **3**, 2191 (1973).
8. V. Yu. Irkhin and M. I. Katsnelson, Fizika Tverdogo Tela **25**, 3383 (1983) [Engl. Transl.: Sov. Phys. - Solid State **25**, 1947 (1983)]; J. Phys. C **18**, 4173 (1985).
9. Y. Nagaoka, Phys. Rev. **147**, 392 (1966).
10. M. I. Auslender and V. Yu. Irkhin, J. Phys. C **18**, 3533 (1985).
11. V. Yu. Irkhin and M. I. Katsnelson, J. Phys.: Condens. Matter **2**, 7151 (1990).
12. V. Yu. Irkhin, M. I. Katsnelson, and A. V. Trefilov, Physica C **160**, 397 (1989); Zh. Eksp. Theor. Fiz. **105**, 1733 (1994) [Sov. Phys. JETP **78**, 936 (1994)].
13. M. I. Katsnelson and D. M. Edwards, J. Phys.: Condens. Matter **4**, 3289 (1992).
14. S. D. Kevan, *Angle-Resolved Photoemission: Theory and Current Applications* (Elsevier, Amsterdam, 1992).
15. R. Wiesendanger, H.-J. Guentherodt, G. Guentherodt, R.J. Cambino, and R. Ruf, Phys. Rev. Lett. **65**, 247 (1990).
16. L. Chioncel, M. I. Katsnelson, R. A. de Groot, and A. I. Lichtenstein, Phys. Rev. B **68**, 144425 (2003).
17. V. Yu. Irkhin and M. I. Katsnelson, Eur. Phys. J. B **19**, 401 (2001).
18. S. V. Vonsovsky, *Magnetism* (Wiley, New York, 1974), vol. 2.
19. M. I. Auslender and V. Yu. Irkhin, Z. Phys. B **56**, 301 (1984).
20. K.-I. Kobayashi, T. Kimura, H. Sawada, K. Terakura, and Y. Tokura, Nature **395**, 677 (1998).
21. J. Unguris, A. Seiler, R. J. Celotta, D. T. Pierce, P. D. Johnson and N. V. Smith, Phys. Rev. Lett. **49**, 1047 (1982).
22. E. Kisker, G. Baum, A. Mahan, W. Raith and B. Reihl, Phys.Rev.B **18**, 2256 (1978).
23. M. J. Otto, R. A. M. van Woerden, P. J. van der Valk, J. Wijngaard, C. F. van Bruggen, and C. Haas, J. Phys.: Cond. Mat.**1**, 2351 (1989).
24. D. M. Edwards, J. Phys. C **16**, L327 (1983).
25. M. I. Auslender and V. Yu. Irkhin, Sol. State Commun. **50**, 1003 (1984).
26. R. Skomski and P. A. Dowben, Europhys. Lett. **58**, 544 (2002).
27. G. A. de Wijs and R. A. de Groot, Phys. Rev. B **64**, 020402 (2001).
28. R. Weht and W. E. Pickett, Phys. Rev. B **60**, 13006 (1999).
29. T. Shishidou, A. J. Freeman, and R. Asahi, Phys. Rev. B **64**, 180401 (2001).
30. I. Galanakis, P. H. Dederichs, and N. Papanikolaou, Phys. Rev. B **66**, 134428 (2002).
31. M. A. Korotin, V. I. Anisimov, D. I. Khomskii, and G. A. Sawatzky, Phys. Rev. Lett. **80**, 4305 (1998).
32. V. I. Anisimov, A. I. Poteryaev, M. A. Korotin, A. O. Anokhin, and G. Kotliar, J. Phys.: Condens. Matter **9**, 7359 (1997).
33. A. I. Lichtenstein and M. I. Katsnelson, Phys. Rev. B **57**, 6884 (1998); M. I. Katsnelson and A. I. Lichtenstein, J. Phys.: Condens. Matter **11**, 1037 (1999).
34. A. Georges, G. Kotliar, W. Krauth, and M. Rozenberg, Rev. Mod. Phys.**68**, 13 (1996).
35. P. Hohenberg and W. Kohn, Phys. Rev. **136**, B864 (1964).
36. W. Kohn and L. J. Sham, Phys. Rev. **140**, A1133 (1965).
37. U. von Barth and L. Hedin, J. Phys. C **5**, 1629 (1972).
38. A. I. Lichtenstein and M. I. Katsnelson, in *Band Ferromagnetism. Ground State and Finite-Temperature Phenomena*, edited by K. Barbeschke, M. Donath, and W. Nolting, Lecture Notes in Physics (Springer-Verlag, Berlin, 2001); A. I. Lichtenstein, M. I. Katsnelson, and G. Kotliar, in: *Electron Correlations and Materials Properties 2*, ed. by A. Gonis, N. Kioussis, and M. Ciftan (Kluwer Academic/Plenum Publishers, 2002).

39. K. Held, I. A. Nekrasov, G. Keller, V. Eyert, N. Bluemer, A. K. McMahan, R. T. Scalettar, T. Pruschke, V. I. Anisimov, and D. Vollhardt, in *Quantum Simulations of Complex Many-Body Systems: From Theory to Algorithms*, edited by J. Grotendorst, D. Marx, and A. Muramatsu, NIC Series, vol. 10 (NIC, Juelich, 2002), p. 175.
40. G. Kotliar and S. Y. Savrasov, in *New Theoretical Approaches to Strongly Correlated Systems*, edited by A. M. Tsvelik (Kluwer Acad. Publ., Dordrecht, 2001).
41. A.V. Zarubin and V.Yu. Irkhin, *Fiz. Tverd. Tela* **41**, 1057 (1999) [*Phys. Solid State*, **41**, 963 (1999)].
42. M. Jarrell, *Phys. Rev. Lett.* **69**, 168 (1992).
43. O. K. Andersen, O. Jepsen, and G. Krier, in *Lectures on Methods of Electronic Structure Calculations*, edited by V. Kumar, O. K. Andersen, and A. Mookerjee (World Scientific, Singapore, 1994), p. 63; O. K. Andersen and T. Saha-Dasgupta, *Phys. Rev. B* **62**, R16219 (2000).
44. L. Vitos, H.L. Skriver, B. Johansson, and J. Kollár, *Comp. Mat. Science* **18**, 24 (2000).
45. L. Chioncel, L. Vitos, I. A. Abrikosov, J. Kollár, M. I. Katsnelson, and A. I. Lichtenstein, *Phys. Rev. B* **67**, 235106 (2003).
46. M. I. Katsnelson and A. I. Lichtenstein, *Eur. Phys. J. B* **30**, 9 (2002).
47. N. E. Bickers and D. J. Scalapino, *Ann. Phys. (N.Y.)* **193**, 206 (1989).
48. V. M. Galitski, *Zh. Eksper. Teor. Fiz.* **34**, 115, 1011 (1958); J. Kanamori, *Prog. Theor. Phys* **30**, 275, (1963).
49. V. I. Anisimov and O. Gunnarsson, *Phys. Rev. B* **43**, 7570 (1991).
50. V. Yu. Irkhin and M. I. Katsnelson, cond-mat/0401625.
51. Yu. M. Yarmoshenko, M. I. Katsnelson, E. I. Shreder, E. Z. Kurmaev, A. Slebarski, S. Plogmann, T. Schlathoelter, J. Braun, and M. Neumann, *Eur. Phys. J. B* **2**, 1 (1998).
52. M. V. Yablonskikh, Y. M. Yarmoshenko, V. I. Grebennikov, E. Z. Kurmaev, S. M. Butorin, L.-C. Duda, J. Nordgren, S. Plogmann, and M. Neumann, *Phys. Rev. B* **63**, 235117 (2001).
53. E. Z. Kurmaev, A. Moewes, S. M. Butorin, M. I. Katsnelson, L. D. Finkelstein, J. Nordgren, and P. M. Tedrow, *Phys. Rev. B* **67**, 155105 (2003).
54. O. Wessely, P. Roy, D. Aberg, C. Andersson, S. Edvardsson, O. Karis, B. Sanyal, P. Svedlindh, M. I. Katsnelson, R. Gunnarsson, D. Arvanitis, O. Bengone, and O. Eriksson, *Phys. Rev. B* **68**, 235109 (2003).
55. G. D. Mahan, *Many-Particle Physics* (Plenum Press, New York, 1990).
56. P. Nozieres and C. T. de Dominicis, *Phys. Rev.* **178**, 1097 (1969).
57. D. N. Zubarev, *Sov. Phys. Uspekhi* **3**, 320 (1960); D. N. Zubarev, *Nonequilibrium Statistical Thermodynamics* (Consultants Bureau, New York, 1974).
58. Yu. A. Izyumov and M. V. Medvedev, *Sov. Phys. - JETP* **32**, 202 (1971).
59. M. I. Auslender, V. Yu. Irkhin, and M. I. Katsnelson, *J. Phys. C* **17**, 669 (1984).
60. A. A. Abrikosov, *Physics* **2**, 5 (1965).
61. H. Suhl, *Phys. Rev.* **138**, A1112 (1965).
62. H. Ebert, *Rep. Progr. Phys.* **59**, 1665 (1996).
63. J. J. Sakurai, *Advanced Quantum Mechanics* (Addison-Wesley, Reading, MA, 1967).
64. F. Gel'mukhanov and H. Agren, *Phys. Rev. A* **49**, 4378 (1994).
65. O. B. Sokolov, V. I. Grebennikov, and E. A. Turov, *phys.stat.sol.(b)* **83**, 383 (1977).

66. M. Rabe, J. Pommer, K. Samm, B. Oezylmaz, C. Koenig, M. Fraune, U. Ruediger, G. Guentherodt, S. Senz, and D. Hesse, *J. Phys.: Condens. Matter* **14**, 7 (2002).
67. C. N. Borca, T. Komesu, H.-K. Jeong, P. A. Dowben, D. Ristoiu, Ch. Hordequin, J. P. Nozieres, J. Pierre, S. Stadler, and Y. U. Idzerda, *Phys. Rev. B* **64**, 052409 (2001).
68. M. Ziese, *Rep. Prog. Phys.* **65**, 143 (2002).
69. E. L. Nagaev, *Phys. Rep.* **346**, 388 (2001).
70. M. Roesler, *phys. stat. sol.* **8**, K31 (1965); F. Hartman-Boutron, *Phys. Kond. Mat.* **4**, 114 (1965).
71. K. Kubo and N. Ohata, *J. Phys. Soc. Japan* **33**, 21 (1972).
72. V. S. Lutovinov and M. Yu. Reizer, *Zh. Eksp. Theor. Fiz.* **77**, 707 (1979).
73. A. P. Grigin and E. L. Nagaev, *phys. stat. sol. (b)* **61**, 65 (1974); E. L. Nagaev, *Physics of Magnetic Semiconductors* (Mir, Moscow, 1983).
74. M. I. Auslender, M. I. Katsnelson, and V. Yu. Irkhin, *Physica B* **119**, 309 (1983).
75. V. Yu. Irkhin and M. I. Katsnelson, *Eur. Phys. J. B* **30**, 481 (2002).
76. R. Kubo, *J. Phys. Soc. Japan* **12**, 570 (1957).
77. H. Nakano, *Prog. Theor. Phys.* **17**, 145 (1957); H. Mori, *Prog. Theor. Phys.* **34**, 399 (1965).
78. N. Furukawa, *J. Phys. Soc. Japan* **69**, 1954 (2000).
79. M. I. Auslender and V. Yu. Irkhin, *Sol. State Commun.* **56**, 703 (1985).
80. E. McCann and V. I. Fal'ko, *Phys. Rev. B* **68**, 172404 (2003).
81. G. Tkachov, E. McCann, and V. I. Fal'ko, *Phys. Rev. B* **65**, 024519 (2001).
82. Y. Meir and N. S. Wingreen, *Phys. Rev. Lett.* **68**, 2512 (1992).
83. M. E. Flatte and G. Vignale, *Appl. Phys. Lett.* **78**, 1273 (2001).